CrossMark

ORIGINAL ARTICLE

Rad-deletion Phenocopies Tonic Sympathetic Stimulation of the Heart

Bryana M. Levitan [1,2] · Janet R. Manning [1,3] · Catherine N. Withers [3] · Jeffrey D. Smith [3] ·
Robin M. Shaw [4] · Douglas A. Andres [3] · Vincent L. Sorrell [2] · Jonathan Satin [1]

Abstract Sympathetic stimulation modulates L-type calcium channel (LTCC) gating to contribute to increased systolic heart function. Rad is a monomeric G-protein that interacts with LTCC. Genetic deletion of Rad ($Rad^{-/-}$) renders LTCC in a sympathomimetic state. The study goal was to use a clinically inspired pharmacological stress echocardiography test, including analysis of global strain, to determine whether $Rad^{-/-}$ confers tonic positive inotropic heart function. Sarcomere dynamics and strain showed partial parallel isoproterenol (ISO) responsiveness for wild-type (WT) and for $Rad^{-/-}$. $Rad^{-/-}$ basal inotropy was elevated compared to WT but was less responsiveness to ISO. Rad protein levels were lower in human patients with end-stage non-ischemic heart failure. These results show that Rad reduction provides a stable inotropic response rooted in sarcomere level function. Thus, reduced Rad levels in heart failure patients may be a compensatory response to need for increased output in the setting of HF. Rad deletion suggests a future therapeutic direction for inotropic support.

Keywords Calcium channel · Echocardiography · Calcium · Cell shortening · Beta-adrenergic stimulation · Heart function

Associate Editor Enrique Lara-Pezzi oversaw the review of this article

✉ Jonathan Satin
 jsatin1@uky.edu

1 Department of Physiology, University of Kentucky College of Medicine, 800 Rose St, Lexington, KY 40536-0298, USA

2 Gill Heart Institute, University of Kentucky, Lexington, KY, USA

3 Department of Molecular and Cellular Biochemistry, University of Kentucky, Lexington, KY, USA

4 Cedars-Sinai Heart Institute, Cedars-Sinai Medical Center, University of California Los Angeles, Los Angeles, CA, USA

Abbreviations

β-AR	Beta-adrenergic receptor
EF	Ejection fraction
ISO	Isoproterenol
LTCC	L-type calcium channel
LVEF	Left ventricular ejection fraction
LVID;d	Left ventricular inner dimension diastolic
$Rad^{-/-}$	Genetic global RRAD knockout mouse
SL	Sarcomere length

Introduction

The heart undergoes extensive remodeling during progression from healthy to failing. Pathological features include hypertrophy of cardiac myocytes and excessive deposition of extracellular matrix. At late stages of remodeling, cardiomyocyte hypertrophy is associated with loss of inotropic function. In addition, the failing heart displays non-responsiveness to β-adrenergic receptor (β-AR) agonists. Cardiac fibrosis contributes to arrhythmias and systolic and diastolic dysfunction [1]. Initial responses to pathological stimuli may illuminate compensatory pathways that can be targeted to preserve normal heart function. Limited studies suggested that the protein Rad may decline in human heart failure patients [2], and in mice, decreased Rad levels constitute part of an early response to pressure overload hypertrophy [2]. Genetic deletion of Rad in the mouse ($Rad^{-/-}$) leads to a stable compensatory remodeled heart with improved systolic function [3].

The Rad knockout mouse model presents a unique opportunity to dissect contributions of cellular hypertrophic remodeling, myocardial Ca^{2+} handling, and fibrosis to cardiac function. Rad is a monomeric Ras-related protein expressed in the myocardium [2, 4, 5]. Rad interacts with the L-type Ca^{2+} channel complex (LTCC) [6] and governs LTCC activity [3, 4, 7]. The $Rad^{-/-}$ heart presents a complex cell/molecular phenotype. Deletion of Rad increases LTCC activity [4], and this

increased current along with increased SERCA2a expression lead to increases in SR Ca^{2+} load [3]. At the cellular and ex vivo working heart levels, Rad deletion leads to a sympathomimetic positive inotropic contractile state [4]. $Rad^{-/-}$ cardiomyocytes are hypertrophied, and the $Rad^{-/-}$ myocardium displays increased fibrosis [3, 8]. $Rad^{-/-}$ hearts showed no evidence of arrhythmogenesis [4], and Rad deletion preserves systolic heart function well into senescence [3]. Taken together, these findings suggest that decreased Rad levels impart stable compensatory inotropic function in response to increased preload and afterload in the failing heart.

Echocardiography is a proven tool for non-invasively assessing heart function in vivo. LV ejection fraction (EF) reduction reflects global LV systolic dysfunction. EF is known to occur late after disease onset, is not an early indicator, and is a prognostic indicator. Speckle-tracking image analysis allows for more sensitive and accurate assessment of function. In animal models, abnormal strain is an early indicator of pathology that precedes fibrosis and systolic dysfunction [9, 10].

We were motivated to further evaluate $Rad^{-/-}$ myocardial function beyond ejection fraction and wall dimensions. Initial studies associated Rad deletion with dysfunction [2, 8, 11], and by association, a study on aging inferred that increases of Rad preserve heart function during senescence [12]. By contrast, our recent studies suggest that Rad deletion preserves function during aging. In this study, we used speckle-tracking-based global strain to test the hypothesis that Rad deletion is beneficial for the heart. We incorporated an acute isoproterenol (ISO) stress test that supports preservation of aspects of non-failing βAR signaling in $Rad^{-/-}$ hearts.

Materials and Methods

Animals

Global *RRAD* null male mice ($Rad^{-/-}$) were generated as previously described [4]. Age-matched in-house bred C57/Bl6 mice (wild-type, WT) served as controls. Male adult mice (3–4 months) and aged mice (>18 months) were evaluated. The experimental procedures and methods used were approved by the Animal Care and Use Committee of the University of Kentucky, and conformed to the NIH Guide for Care and Use of Laboratory Animals.

Ventricular Myocyte Isolation

Adult ventricular myocyte isolation was performed as in previous studies [4]. Prior to heart excision, mice were anesthetized with ketamine + xylazine (90 + 10 mg/kg intraperitoneal). The hearts were excised from adult $Rad^{-/-}$ and wild type mice and immediately perfused on a Langendorff apparatus

with a high-potassium Tyrode buffer and then digested with 5 to 7 mg liberase (Roche). After digestion, the atria were removed and ventricular myocytes were mechanically dispersed. Calcium concentrations were gradually restored to physiological levels in a stepwise fashion, and only healthy quiescent ventricular myocytes were used for electrophysiological analysis or calcium imaging within 12 h.

For simultaneous measurement of cytosolic calcium and sarcomere length, isolated ventricular myocytes were loaded with cell permeable Fura-2 AM at room temperature for 5 min, washed, and re-suspended in physiological saline solution (PSS) containing 1.8 mM calcium. Myocytes were then field stimulated at 1 Hz, and the $F_{340/380}$ ratio was measured as an indicator of changes in cytosolic calcium concentration. For ISO measurements, cells were paced for 2 min prior to recording in PSS containing 100 nM isoproterenol. Optical imaging of sarcomere frequency was analyzed and converted into sarcomere length using Ion Wizard software (IonOptix, Westwood, MA).

Echocardiography

Transthoracic echocardiography was performed using the Visual Sonics 770 imaging system (Toronto, Canada) equipped with 30-MHz probe. Mice underwent transthoracic echocardiography, under light anesthesia (inhaled isoflurane 1–2%), with heart rate (350–500 beats per minute) and core temperature (37 °C) continuously monitored. The heart was visualized in 2D from modified parasternal long axis, short axis, and apical views. The left ventricular dimensions and calculated left ventricular EF were measured from the short axis M-mode display. Left ventricular systolic strain was derived from the Visual Sonics software-utilizing speckle tracking of the modified parasternal long axis and short axis images. All measurements were obtained in triplicate and averaged. The sonographer was blinded to animal genotype, and data analysis was performed with animal genotype blinded.

For the pharmacological stress test, a single I.P. injection of isoproterenol (ISO, 30 mg/kg, USP) was given immediately after baseline echocardiography measures were recorded. Heart rate was monitored; within 5 min, a heart rate increase; confirmed drug effect and echocardiography measures were repeated (marked ISO in graphs).

Human Heart: Patient Tissue

De-identified human heart lysates from individuals without heart failure and with end-stage non-ischemic dilated cardiomyopathy were obtained from the Cedars-Sinai Heart Institute Biobank. Heart failure tissue was obtained from the hearts removed at the time of transplant, and non-failing tissue was

obtained from previously healthy organ donors whose hearts were not transplanted for technical reasons. For each heart, cold cardioplegia was perfused antegrade prior to cardiectomy, and the explanted heart was placed immediately in ice-cold physiologic solution. Full-thickness samples from the free wall of the left ventricle were cleaned rapidly of all epicardial fat, and aliquoted into cryovials, which were submerged in liquid N2 to snap-freeze before storage at −80 °C.

Western Blotting

For protein lysate preparation, 100 mg of ventricular tissues were homogenized in 1 ml RIPA buffer, followed by sonication and centrifugation at 10,000 g for 20 min at 4 °C. Protein concentration in the clarified lysates was determined using the BioRad DC Protein Assay and normalized. Human heart homogenates were diluted in SDS sample buffer and loaded into a 10% Criterion Tris–HCl StainFree gel (BioRad) at 30 µg per lane. Individual heart lysates were normalized to total protein (Fig. 1c) as measured with Image Lab software (BioRad) prior to transfer onto Protran nitrocellulose membrane (Amersham). The membrane was blocked in TBS with 5% dry milk and

0.1% Tween20 before incubation with goat anti-Rad primary antibody (Everest Biosciences EB11418, 1:1000). Following washes and incubation with HRP-conjugated rabbit anti-goat secondary antibody (Jackson Immunochemicals), the blot was developed with SuperSignal West Pico (Thermo Scientific) and visualized on a ChemiDoc MP (BioRad). Image Lab was used to quantify band intensities, and the data were analyzed by *t* test in GraphPad Prism.

Run to Exhaustion, Exercise Tolerance Test

Mice ran on a 6-lane powered treadmill (Exer3/6, Columbus Instruments, Columbus, OH) using a protocol modeled from reference [13]. A two-day acclimatization period consisted of 5 m/min for 5 min on day 1. The day 2 protocol was a 3-min stationary period, followed by 5 m/min for 5 min with speed gradually increased to 21 m/min for an additional 15 min. If mice stopped running, they were gently patted on the hindquarters. Mice that refused to run during day 2 were excluded from analysis. For the exercise tolerance test on day 3, mice were run until they reached volitional exhaustion. Treadmill speed was gradually increased to 21 m/min; this pace was

Fig. 1 Global systolic strain is enhanced in adult Rad$^{-/-}$. **a** Representative echocardiographic images showing raw strain data for WT and Rad$^{-/-}$ for longitudinal plane (*left*) and circumferential plane (*right*). **b** Pooled data for longitudinal strain. Aging decreased global longitudinal strain in WT (−18.7 ± 1.7% in adult versus −10.8 ± 1.9% in aged WT; $p < 0.01$). **c** Pooled data for circumferential strain. Rad deletion significantly enhances circumferential strain for adult and during aging compared to WT (for adult: strain = −19.9 ± 1.3% versus −27.2 ± 1.0, for WT and Rad$^{-/-}$, respectively; $p < 0.001$; for aged: strain = −17.8 ± 0.7 versus −23.2 ± 0.7, for WT and Rad$^{-/-}$, respectively; $p < 10^{-4}$

J. of Cardiovasc. Trans. Res. (2016) 9:432–444

435
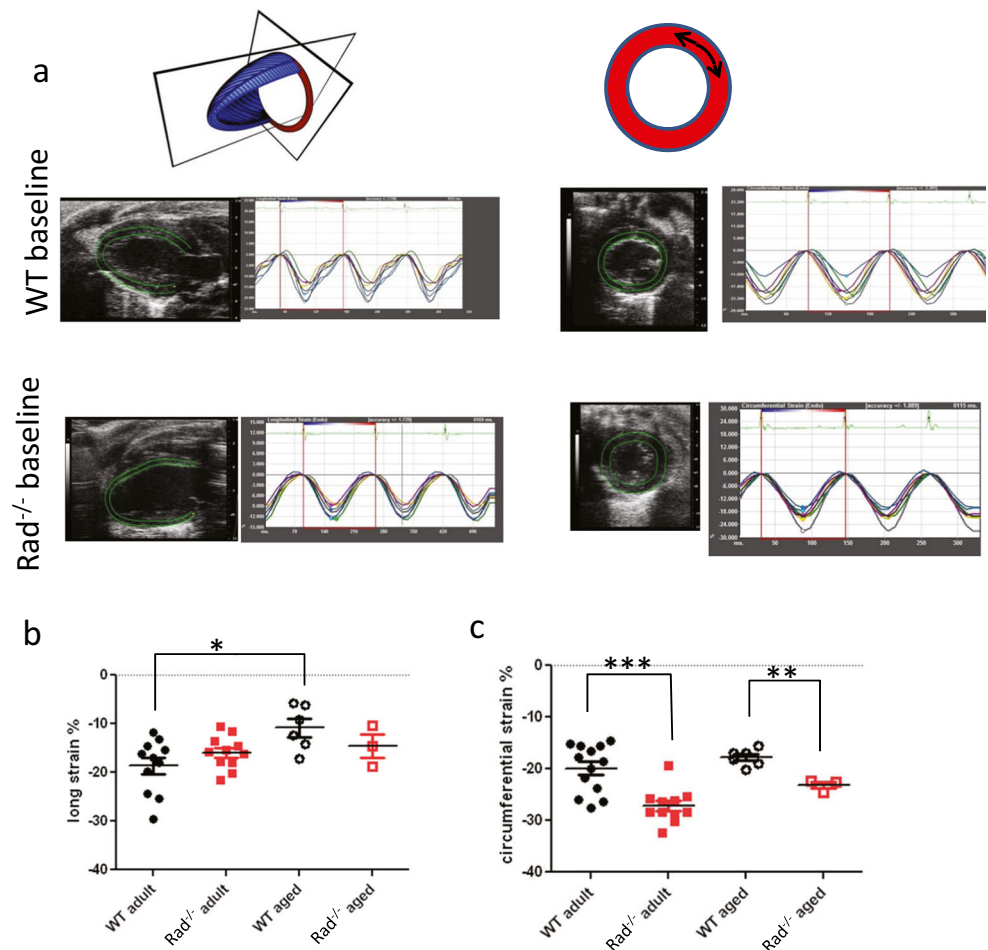
maintained until exhaustion. Exhaustion was defined as failure to keep up with treadmill despite hindquarter prods. Time to exhaustion was recorded and plotted. Investigators were blinded to mouse genotype.

Statistics

Data are presented as mean ± standard error of the mean. Tests for effects of genotype and aging were made on independent groups and evaluated with one-way analysis of variance (ANOVA) and post-hoc Tukey tests. For ISO stress test measurements, the difference of ISO and baseline for each sample was evaluated for t tests for a difference = 0. Additionally, a two-way ANOVA was applied to data to analyze interactions, ISO, and genotype effects. $p < 0.05$ was considered statistically significant. We used GraphPad Prism v6.0 (San Diego, Ca).

Results

Rad$^{-/-}$ Hearts Exhibit Canonical Hypertrophic Remodeling Markers but Maintain Preserved Systolic and Diastolic Function in Aging

The Rad$^{-/-}$ mouse heart presents with increased fibrosis [3, 8] and thicker ventricular walls, but preserved E/A ratio [3]. These contradictory findings motivated us to perform a more in-depth examination of the Rad$^{-/-}$ heart. Strain is an early indicator of LV systolic dysfunction. We therefore used speckle-tracking echocardiography to evaluate global and regional strain in WT and Rad$^{-/-}$ in adult and aged mice (Fig. 1a). Global longitudinal strain was not significantly different in adult. With aging, there was a significant decline in WT, but not in Rad$^{-/-}$ (Fig. 1b). Global circumferential strain showed more discrete changes between WT and Rad$^{-/-}$. Adult global circumferential strain was significantly greater in Rad$^{-/-}$ compared to WT in adult and aged mice (Fig. 1c).

Figure 2a shows heart orientation juxtaposed to a schematic for evaluating regional strain. Regional longitudinal strain was not different between WT and Rad$^{-/-}$ in adult or with aging except for the basal inferior-lateral region (Fig. 2b). By contrast, for all regions of circumferential strain, mean values were greater in Rad$^{-/-}$ than in WT in adult and aging (Fig. 2c). Three regions, the anterior-lateral, inferior-lateral, and anterior-septal regions, reached statistical significance (Fig. 2c). With aging, the spread between mean values reduced suggesting that Rad$^{-/-}$ heart function was maintained but susceptible to aging-induced decline of function. The important point is that despite increased fibrosis and remodeled LV, Rad deletion preserves many detectable aspects of LV function in adult.

ISO Response In Vivo

We performed an ISO stress test paradigm for echocardiography inspired by the clinical stress test (for patients unable to exercise) to reveal deficits in function triggered by heart remodeling. Adult mice were imaged at baseline and acutely administered ISO. Within 5 min, HR was elevated and the hearts were re-imaged. Ejection fraction was significantly increased by ISO in WT (59.5 ± 0.6% at baseline; 92.8 ± 1.7% ISO; Fig. 3a). The ISO effect on EF was greater for WT than that for Rad$^{-/-}$ (mean difference 33.3 ± 1.8 versus 7.4 ± 1.1%, for WT and Rad$^{-/-}$, respectively; Fig. 3b). EF plotted as a function of HR showed a weak relationship, but linear regression analysis did not indicate a slope significantly different from zero (Fig. 3c). Thus, EF increases are independent of HR over the range of HR measured. Maximal LV diastolic chamber dimensions (LVID;d) tracked with changes in EF for WT (Fig. 3d). HR did not contribute to ISO-induced decrease of LVID;d (Fig. 3e). The ISO effect to decrease LVID;d was significant for WT but not for Rad$^{-/-}$ (Fig. 3f).

Global longitudinal and circumferential strain were significantly enhanced by ISO for WT, but not for Rad$^{-/-}$ (Fig. 4a–d). Strain is expressed as percent change and therefore can be influenced by changes in chamber dimensions whereby smaller LVID;d results in apparent enhanced strain, all else being equal. Plots of longitudinal and circumferential strain as a function of LVID;d demonstrate that this relationship holds for WT under basal conditions and for Rad$^{-/-}$ for basal and acute ISO (Fig. 4e, f). Regional strain showed non-uniform responses to ISO. Longitudinal regional strain was not affected by Rad deletion but was significantly enhanced by ISO in the posterior base, posterior midwall, anterior midwall, and anterior apical segments (Table 1). The mean circumferential strain for each segment was greater than that for Rad than WT (Table 2). Analysis by segment showed an interaction effect for the lateral region and ISO effects on the anterior free, lateral, and septal segments (Table 2). This regional pattern reflects the left anterior descending coronary artery myocardial distribution [14].

### Sarcomere Length Changes Faster in Rad$^{-/-}$ than in WT

The dynamics of the change in sarcomere length (not overall length per se) translate into myocardial function [15]. It is well-established that small changes in sarcomeric (and cellular) fractional shortening translate into larger changes in heart wall motion, and a primary effect of Rad$^{-/-}$ is to enhance myocardial Ca^{2+} homeostasis that in turn drives sarcomere level function. We therefore analyzed sarcomere velocity in WT and Rad$^{-/-}$. Figure 5a, b plots sarcomere length (SL) along with the rate of change of sarcomere length (Fig. 5c, d) to illustrate sarcomere kinetics. To summarize SL kinetics, we measured the peak velocity of contraction (−dSL/dt; Fig. 5e) and the peak velocity

436

J. of Cardiovasc. Trans. Res. (2016) 9:432–444

Fig. 2 Regional systolic strain analysis: Rad deletion improves strain in selected segments. **a** (*Upper panels*) representative longitudinal axis view (*left*) with schematic showing demarcation of segments (*right*). Abbreviations: *BA-S* basal anterior-septal, *MA-S* mid anterior-septal, *AA* apical anterior, *AL* apical lateral, *MI-L* mid inferior-lateral, *BI-L* basal inferior-lateral. **a** (*Lower panels*) representative short axis view (*left*) with schematic showing demarcation of segments (*right*). Abbreviations: *A* anterior, *AL* anterior lateral, *IL* inferior lateral, *I* inferior, *IS* inferior septal, *AS* anterior septal. **b** Longitudinal segmental strain, pooled data. *$p < 0.01$. **c** Circumferential segmental strain, pooled data
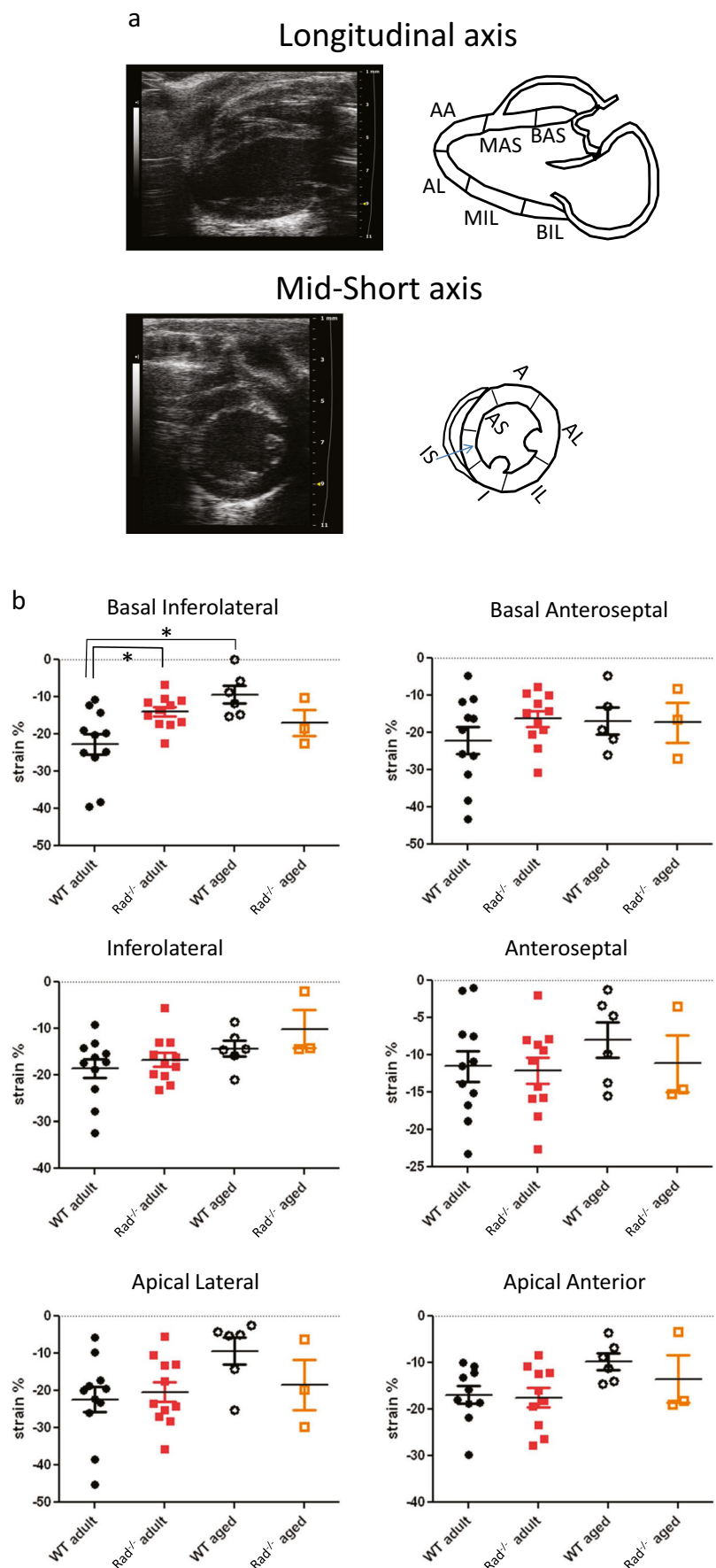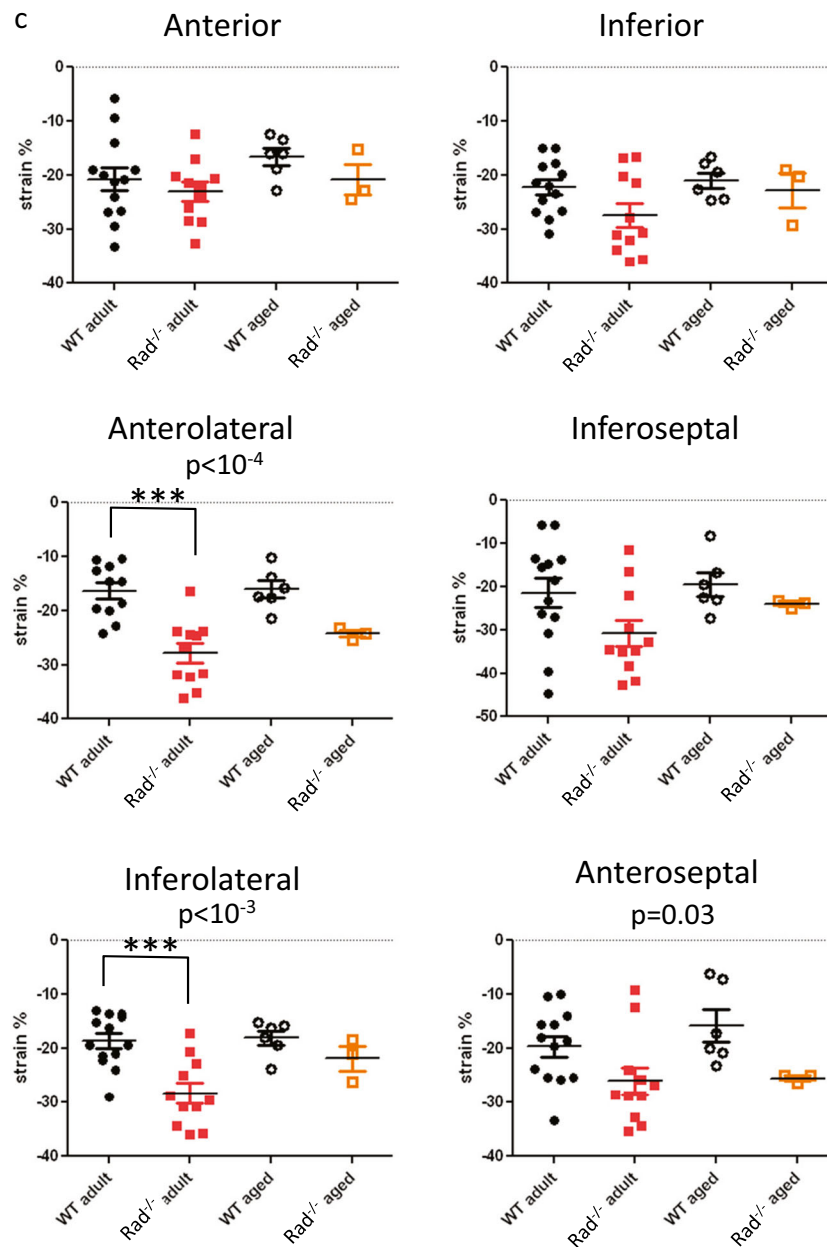
Fig. 2 continued.

of relaxation (+dSL/dt; Fig. 5f). Rad$^{-/-}$ SL relaxation peak velocity was significantly faster than that for WT (2.5 ± 0.3 and 5.3 ± 0.9 μm/s, $p < 0.01$, for Rad$^{-/-}$ and WT, respectively), and contractile kinetics trended towards faster values in Rad$^{-/-}$ (3.7 ± 0.5 and 6.1 ± 0.5 μm/s, $p = 0.08$, for Rad$^{-/-}$ and WT, respectively). These results suggest that in Rad$^{-/-}$ increased Ca^{2+} homeostasis [3, 4] drives faster sarcomere kinetics.

We previously noted that the Rad$^{-/-}$ basal cellular phenotype approximates WT cardiomyocyte properties following ISO modulation [4]. We therefore evaluated SL kinetics response to acute ISO administration. ISO significantly increased SL contractile (Fig. 5g) and relaxation kinetics

(Fig. 5h) in WT but had no effect on Rad$^{-/-}$ cardiomyocytes (Fig. 5i). The ISO-elevated WT kinetics was not different from Rad SL kinetics at baseline.

Rad Levels Decrease in Human Failing Heart

Rad is a member of the RGK subfamily of monomeric G-proteins, and regulation of expression levels is a key defining feature of this protein family [16]. Western blot evaluation of protein levels in human heart shows abundant Rad protein in non-failing control and significantly decreased levels in non-ischemic failing hearts (Fig. 6(a)). Thus, Rad decrease is a

Fig. 3 EF evaluation of ISO stress echocardiography test. **a** Pooled data for ISO-stress test paradigm. ISO significantly elevates EF in WT. ***p < 10^{-3}. **b** Pooled data of ISO difference for each animal. *t* test for difference = 0 was significant for WT and Rad$^{-/-}$. **c** Slopes of EF as a function of HR are not significantly different from zero slope. **d** LVID;d as a function of HR. **e–f** Chamber dimensions with acute ISO. The change of LVID;d for difference = 0, WT p < 10^{-3}; Rad$^{-/-}$, ns, p = 0.06
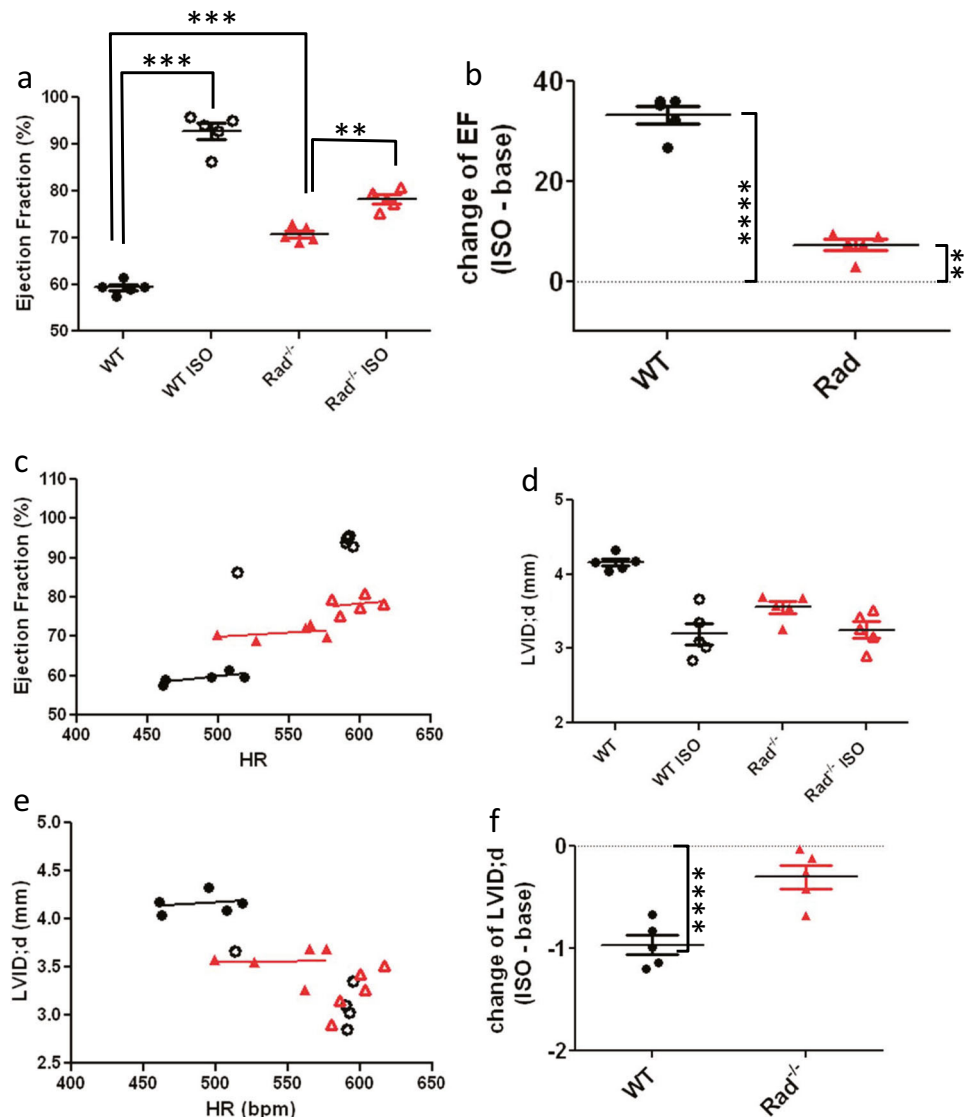
clinically relevant response to pathological stimuli. Heart failure patients respond to the 6-min walk test with significantly reduced exercise tolerance [17]. We therefore subjected mice to an exercise tolerance test. During a run to exhaustion test, there was no significant difference between WT and RadKO (Fig. 6(b)); WT 20.4 ± 3.8 min, n = 9; RadKO 17.3 ± 3.6 min, n = 5). Taken together, these data are consistent with our working hypothesis that decreased levels of Rad contributes to a compensatory response to preserve heart function.

Discussion

Echocardiography permits non-invasive evaluation of real-time cardiac function, and strain analysis provides a sensitive, early index of alterations of cardiac mechanics in advanced clinical practice [18–20] and in mice [9, 21, 22]. In this study,

we show that Rad level decreases in human heart failure, and that Rad deletion in mice results in beneficial heart function. These findings suggest that Rad downregulation in human heart failure may contribute to compensatory beneficial function. Rad deletion shows no age-related decline of myocardial performance and improved global strain. Rad$^{-/-}$ mice have enhanced Ca^{2+} homeostasis [4, 7] that in turn can drive sarcomere dynamics to ultimately drive cardiac mechanics [15]. We now show evidence that faster sarcomere kinetics in Rad$^{-/-}$ are associated with improved in vivo cardiac performance and mechanics. The in vivo heart mechanics response to ISO parallels that of SL dynamics consistent with a mechanism of action whereby Rad deletion mimics tonic sympathetic activation, yet without deleterious consequences.

The pharmacological stress echocardiography test is a mainstay diagnostic tool for unmasking heart functional deficits in patients with coronary artery disease. Despite

Fig. 4 Global strain is increased by ISO and is elevated in baseline for Rad$^{-/-}$ compared to WT. **a** Pooled data global longitudinal strain for ISO-stress test paradigm. ISO significantly elevates global longitudinal strain in WT but not Rad$^{-/-}$. **b** Pooled data of ISO difference for each animal. t test for difference $= 0$ was significant for WT and Rad$^{-/-}$. *$p = 0.01$. **c** Pooled data global circumferential strain for ISO-stress test paradigm. ISO significantly elevates global longitudinal strain in WT but not Rad$^{-/-}$. **d** Pooled data of ISO difference for each animal. t test for difference $= 0$ was significant for WT only. **$p < 0.01$. **e, f** Longitudinal (E) and circumferential (F) strain as a function of LVID;d. *Straight lines are linear regression fit*
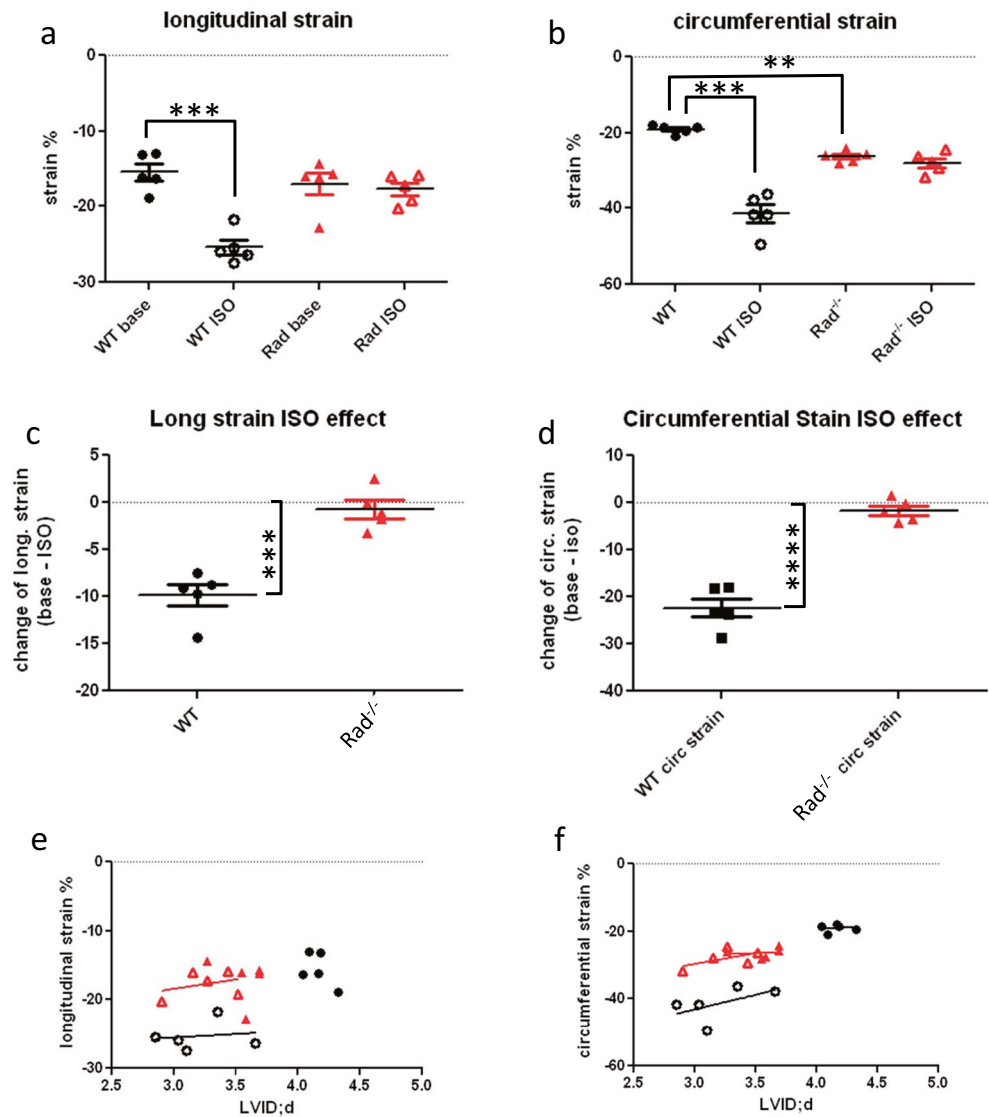
its widespread use in patients, there have been few applications in mice. By contrast to echocardiography, acute ISO challenge is widely used at the cellular and ex vivo heart levels to explore myocardial function. Specifically with regard to the effects of Rad, L-type Ca^{2+} current (I$_{Ca,L}$) demonstrates a ceiling effect with Rad knockout

Table 1 Longitudinal regional strain: source of variation long axis (two-way ANOVA)

	Interaction			ISO effect			RadKO effect		
	% total variation	p value		% total variation	p value		% total variation	p value	
Basal infero-lateral	12.2	0.07	ns	24.0	0.02	*	0.5	0.76	ns
Inferior lateral	6.3	0.16	ns	31.0	0.008	**	20.4	0.03	*
Apical lateral	15.1	0.009	**	26.0	0.002	**	9.4	0.20	ns
Basal antero-septal	26.4	0.002	**	21.2	0.003	**	7.2	0.24	ns
Mid antero-septal	24.1	0.03	*	12.0	0.09	ns	19.2	0.02	*
Apical anterior	16.4	0.02	*	26.3	0.007	**	2.3	0.51	ns

ns not significant; *$p < 0.05$; **$p < 0.01$

Table 2 Circumferential regional strain: source of variation short axis (two-way ANOVA)

	Interaction			ISO effect			RadKO effect		
	% total variation	p value		% total variation	p value		% total variation	p value	
Anterior	0	0.94	ns	12.3	0.03	*	5.0	0.29	ns
Antero-lateral	12.7	0.03	*	25.7	0.005	**	2.0	0.43	ns
Inferior lateral	1.8	0.44	ns	10.6	0.08	ns	5.6	0.34	ns
Inferior	0.2	0.83	ns	2.8	0.4	ns	0	0.97	ns
Inferior-septal	10.8	0.10	ns	26.7	0.02	*	0.9	0.50	ns
Antero-septal	2.1	0.36	ns	15.3	0.02	*	4.6	0.34	ns

ns not significant

[4] or knockdown [7]. "Ceiling effect" is defined here as baseline measures that are elevated and are not different from WT measures that were maximally stimulated by ISO. Our previous studies showed that in Rad$^{-/-}$ myocyte Ca^{2+} amplitude and fractional cellular shortening also shows a ceiling effect [4]. In the present study, we now show that SL velocity and LVID;d similarly exhibit the ceiling effect with an ISO stress test. By contrast, the rates of developed pressure and relaxation in the working heart tracks with EF obtained from echo ISO stress test. Depending on parameters measured, four patterns emerge for myocardial responsiveness to the ISO stress test: (1) ceiling effect; (2) WT at baseline <Rad$^{-/-}$ baseline but WT + ISO > Rad$^{-/-}$ + ISO; (3) WT at baseline <Rad$^{-/-}$ baseline but WT + ISO > Rad$^{-/-}$ + ISO, with no Rad$^{-/-}$ + ISO response; and (4) WT ≈ Rad$^{-/-}$. The first scenario, the ceiling effect fits with a wealth of data biochemically localizing Rad to the LTCC complex where its absence instigates a βAR-like modulated I$_{Ca,L}$ [3, 4, 7]. Consequently, βAR modulated I$_{Ca,L}$ provides more trigger Ca^{2+} for Ca^{2+}-induced Ca^{2+} release logically leading to increased Ca^{2+} transients, cell shortening, and SL velocities. Correspondence of ceiling effect of these cellular/molecular properties with diastolic chamber dimensions suggests that Ca^{2+} homeostasis via LTCC contributes to stress-modified LVID;d. Scenario #4 (WT ≈ Rad$^{-/-}$) is thus far limited to Ca^{2+} re-uptake and may be attributable to increased SERCa2 in Rad$^{-/-}$ [3]. This is important because it shows that Rad$^{-/-}$ myocardium retains βAR responsiveness which is a contraindication to failing myocardium.

EF and global systolic strain do not follow a ceiling effect for Rad$^{-/-}$, but a difference between WT and Rad$^{-/-}$ in ISO response is still observed. EF and global systolic strain on first glance show mean values for ISO stimulation whereby WT exceeds Rad$^{-/-}$ function. EF obtained from 2D echocardiography is defined by the ratio of LV inner dimensions at systole and diastole. As noted above, diastolic chamber dimensions show a ceiling effect for ISO stress test for Rad$^{-/-}$. Therefore, apparent gain in function

for WT must come from differential responsiveness to systolic function as suggested by cellular/molecular studies. Perhaps of prime importance is that the relatively minor response of Rad$^{-/-}$ in the ISO stress test is not indicative of myocardial detrimental function, rather is secondary to augmented baseline function.

Strain was not changed by ISO in contrast the EF response. LV inner dimension in diastole is an important contributor to strain. Global systolic strain is a fractional change in stretch; therefore, all else being equal, the smaller the starting dimensions, the greater the absolute value of strain value is recorded. Indeed our data suggests that the plot of strain as a function of LVID;d showed that Rad$^{-/-}$ and Rad$^{-/-}$ + ISO can linearly extrapolate to WT strain. ISO significantly increased global strain independent of LVID;d in WT. The absence of ISO effect on Rad genotype is a consequence of ceiling effect. Apparent lack of change of strain for Rad$^{-/-}$ + ISO relative that of WT + ISO may simply reflect the small LVID;d of Rad$^{-/-}$. In summary, proper interpretation of strain values must include assessment of LVID;d. This is especially important in rodent models of disease that alter cardiac dimensions with time.

Strain is an early and sensitive indicator of LV global and regional systolic dysfunction, [10, 23, 24] and one goal of this study was to assess whether prior studies overlooked early indicators of loss of function in the Rad$^{-/-}$ heart. The Rad$^{-/-}$ heart exhibits increased fibrosis [2, 3, 8] yet improved EF. This raises two questions contemporaneously: (1) Given that the presence of fibrosis associates with pathology was an early event in heart dysfunction overlooked in earlier studies? and (2) Does the tonic elevated Ca^{2+} handling in Rad$^{-/-}$ drive pathological function? Circumferential strain is useful here as an early measure that tracks with pathological heart remodeling following trans-aortic constriction in mice. Concurrent with fibrosis, speckle-tracking echocardiography showed declining circumferential strain [25]. Myocardial Ca^{2+} homeostasis is a focal point for increasing the inotropic response, yet increased Ca^{2+} can also contribute to

Fig. 5 Rad$^{-/-}$ sarcomere dynamics is faster, and Rad$^{-/-}$ basal SL kinetics is indistinguishable from ISO stimulated WT SL kinetics (ceiling effect). **a** Representative SL trace for one beat from WT and **b** from Rad$^{-/-}$ cardiomyocyte. Cells were paced to steady state at 1 Hz. 1 s total time showed. **c** 1 s derivative of SL for WT and **d** for Rad$^{-/-}$. *Inset*: normalized superimposed Ca^{2+} transient and SL traces. *Scale bar* = 0.3 fluorescence units for Ca^{2+} transient, SL trace from main panel normalized to peak Ca^{2+}. No time *scale bar*, the peak to peak interval is 1 s. **e** Pooled peak SL velocity for contraction and **f** for relaxation. **p < 0.001. **g**, **h** ISO speeds sarcomere relaxation velocity (A) and contraction velocity (B) in WT. See Table 1 for statistical analysis of panels **a** and **b**. **i** Pooled data of ISO difference for each cardiomyocyte. *t* test for difference = 0 was significant for WT for relaxation and contraction in WT but not significant for Rad$^{-/-}$. *p < 0.02
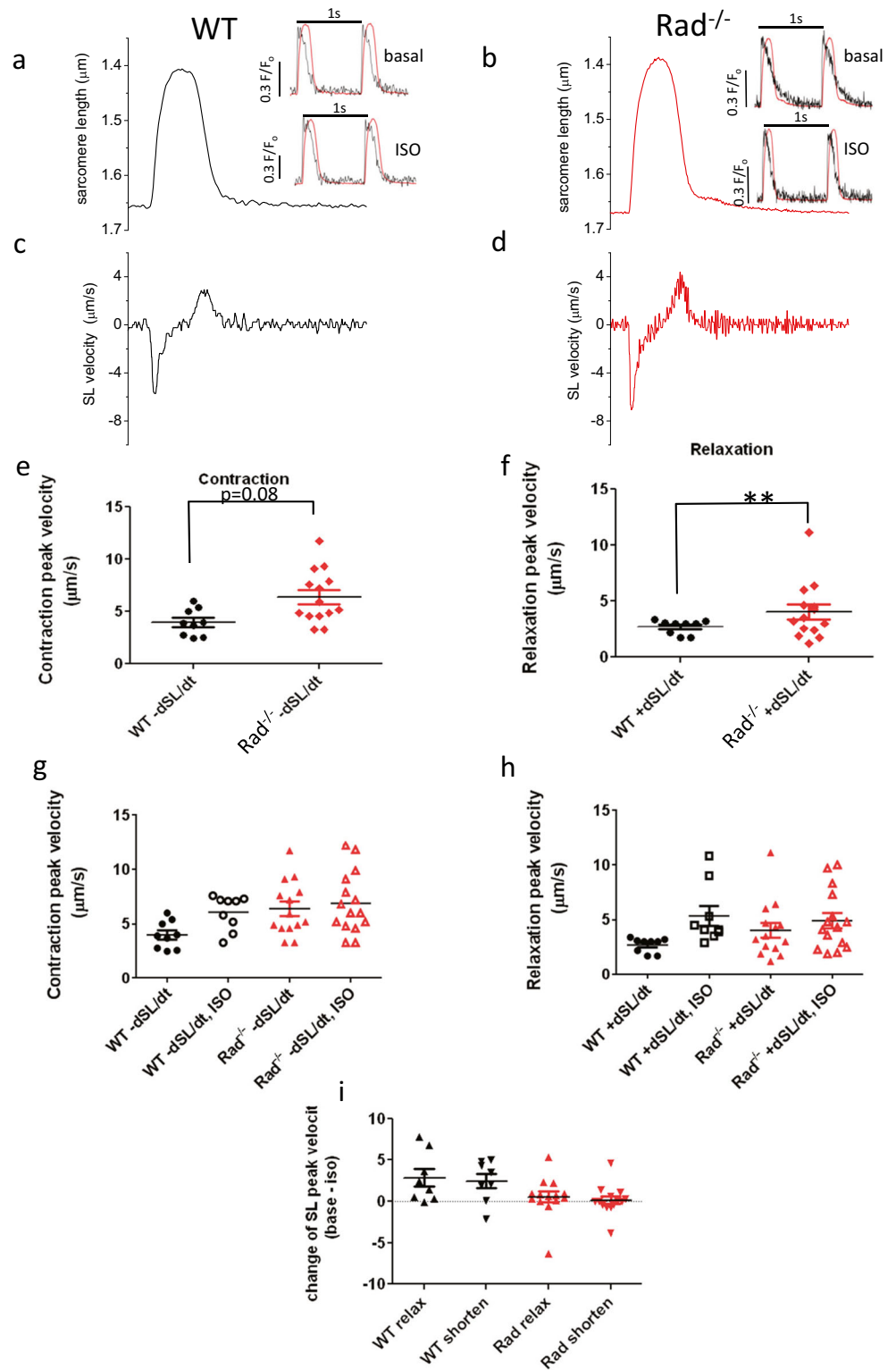
pathological remodeling via signaling cascades culminating in altered transcriptional regulation [26, 27]. Forced over-expression of Ca$_V$1.2, the LTCC pore-forming channel subunit leads to a long-term, slow, progressive pathological remodeling [28]. Ca$_V$β2 over-expression induces more rapid onset heart failure model [29]. By
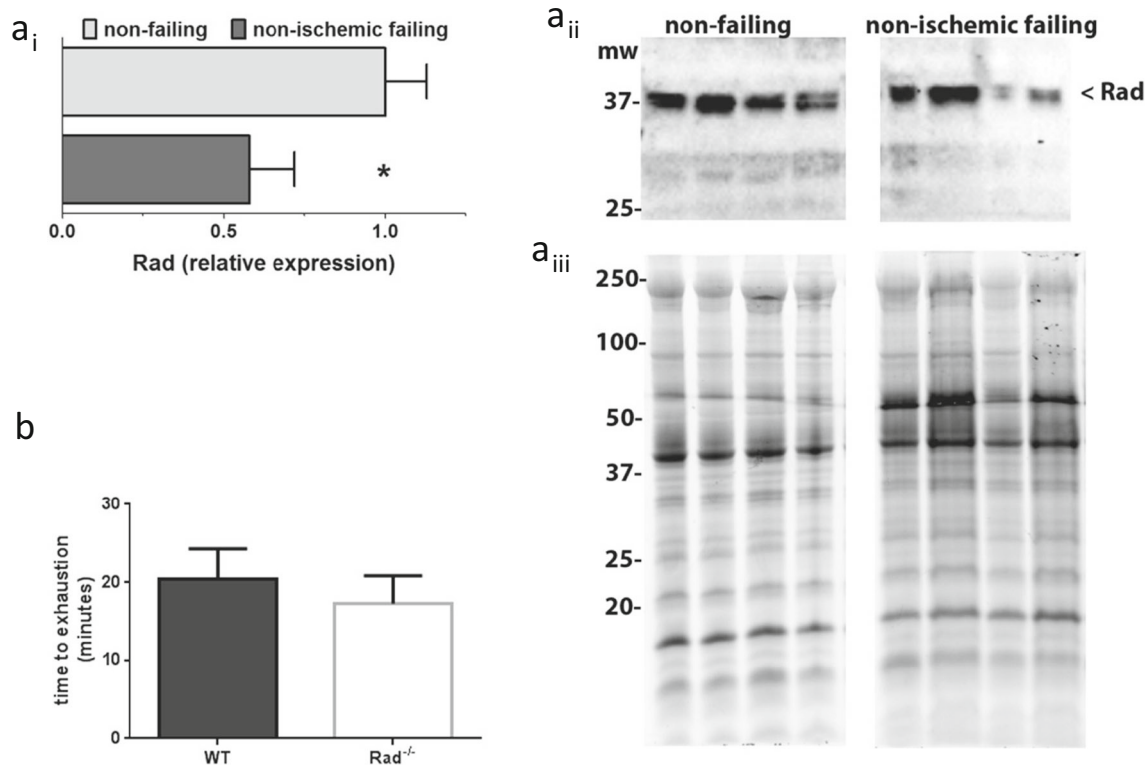
Fig 6 Rad protein levels are downregulated in human failing heart. a_i Rad protein is reduced by 40% in non-ischemic heart failure. (*$p < 0.05$ by t test, $n = 8$ non-failing and nine non-ischemic failing). a_{ii} Representative immunoblot of Rad in human heart failure. a_{iii} Total protein was assessed using stain-free enabled imaging. b Exercise tolerance test shows no significant difference between WT and RadKO

contrast, Rad deletion elevates LTCC activity with a beneficial stable compensatory state [3]. Therefore, it was important to perform a deeper probe of the question whether early indicators of cardiac dysfunction present in Rad$^{-/-}$ given the incomplete overlapping signaling pathways among Rad$^{-/-}$, Ca$_V$1.2-, and Ca$_V\beta$2 over-expression. One key distinction is that Rad$^{-/-}$ shows elevated SERCa2 and increased sarcoplasmic reticulum Ca^{2+} load [3]; each of these findings is counterfactual to canonical heart failure phenotypes [30] but does associate with endurance training [31].

In summary, Rad deletion induces positive under resting conditions. Rad$^{-/-}$ heart dimensions exhibit smaller chamber dimensions but with increased contractility. Clinically inspired pharmacological stress echocardiography testing in mice reveals that ISO-stimulated EF is greater in WT than in Rad$^{-/-}$, and systolic strain is not influenced by ISO. Although tonic elevated Ca^{2+} can lead to deleterious myocardial remodeling, preserved systolic strain in Rad$^{-/-}$ supports the idea that reduction in Rad levels, such as observed in heart failure patients, comprises a stable compensatory response to boost resting cardiac output. In addition, Rad$^{-/-}$ hearts have significantly increased fibrosis but retain normal to improved myocardial function. We conclude

that targeting Rad reduction is a potential future therapeutic target for treating systolic heart failure and contributes to overcoming the negative mechanical consequences imposed by fibrosis.

Compliance with Ethical Standards

References

1. Rockey, D. C., Bell, P. D., & Hill, J. A. (2015). Fibrosis—a common pathway to organ injury and failure. *New England Journal of Medicine, 372*(12), 1138–1149. doi:10.1056/NEJMra1300575.

2. Chang, L., Zhang, J., Tseng, Y. H., Xie, C. Q., Ilany, J., Bruning, J. C., et al. (2007). Rad GTPase deficiency leads to cardiac hypertrophy. *Circulation, 116*(25), 2976–2983. doi:10.1161/CIRCULATIONAHA.107.707257.

3. Manning, J. R., Withers, C. N., Levitan, B., Smith, J. D., Andres, D. A., & Satin, J. (2015). Loss of Rad-GTPase produces a novel adaptive cardiac phenotype resistant to systolic decline with aging. *American Journal of Physiology - Heart and Circulatory Physiology, 309*(8), H1336–H1345. doi:10.1152/ajpheart.00389.2015.

4. Manning, J. R., Yin, G., Kaminski, C. N., Magyar, J., Feng, H. Z., Penn, J., et al. (2013). Rad GTPase deletion increases L-type Calcium channel current leading to increased cardiac contraction. *Journal of the American Heart Association, 2*(6), doi:10.1161/jaha.113.000459.

5. Hawke, T. J., Kanatous, S. B., Martin, C. M., Goetsch, S. C., & Garry, D. J. (2006). Rad is temporally regulated within myogenic progenitor cells during skeletal muscle regeneration. *American Journal of Physiology - Cell Physiology, 290*(2), C379–C387. doi:10.1152/ajpcell.00270.2005.

6. Finlin, B. S., Crump, S. M., Satin, J., & Andres, D. A. (2003). Regulation of voltage-gated calcium channel activity by the Rem and Rad GTPases. *PNAS, 100*, 14469–14474. doi:10.1073/pnas.2437756100.

7. Wang, G., Zhu, X., Xie, W., Han, P., Li, K., Sun, Z., et al. (2010). Rad as a novel regulator of excitation-contraction coupling and beta-adrenergic signaling in heart. *Circulation Research, 106*(2), 317–327. doi:10.1161/CIRCRESAHA.109.208272.

8. Zhang, J., Chang, L., Chen, C., Zhang, M., Luo, Y., Hamblin, M., et al. (2011). Rad GTPase inhibits cardiac fibrosis through connective tissue growth factor. [Journal Article]. *Cardiovascular Research, 91*, 90–98. doi:10.1093/cvr/cvr068.

9. Shepherd, D. L., Nichols, C. E., Croston, T. L., McLaughlin, S. L., Petrone, A. B., Lewis, S. E., et al. (2016). Early detection of cardiac dysfunction in the type 1 diabetic heart using speckle-tracking based strain imaging. *Journal of Molecular and Cellular Cardiology, 90*, 74–83. doi:10.1016/j.yjmcc.2015.12.001.

10. Shah, S. J., Aistrup, G. L., Gupta, D. K., O'Toole, M. J., Nahhas, A. F., Schuster, D., et al. (2014). Ultrastructural and cellular basis for the development of abnormal myocardial mechanics during the transition from hypertension to heart failure. *American Journal of Physiology. Heart and Circulatory Physiology, 306*(1), H88–100. doi:10.1152/ajpheart.00642.2013.

11. Yada, H., Murata, M., Shimoda, K., Yuasa, S., Kawaguchi, H., Ieda, M., et al. (2007). Dominant negative suppression of Rad leads to QT prolongation and causes ventricular arrhythmias via modulation of L-type Ca2+ channels in the heart. *Circulation Research, 101*(1), 69–77. doi:10.1161/CIRCRESAHA.106.146399.

12. Flynn, J. M., O'Leary, M. N., Zambataro, C. A., Academia, E. C., Presley, M. P., Garrett, B. J., et al. (2013). Late-life rapamycin treatment reverses age-related heart dysfunction. *Aging Cell, 12*(5), 851–862. doi:10.1111/acel.12109.

13. Davidson, S. R., Burnett, M., & Hoffman-Goetz, L. (2006). Training effects in mice after long-term voluntary exercise. *Medicine and Science in Sports and Exercise, 38*(2), 250–255. doi:10.1249/01.mss.0000183179.86594.4f.

14. Mor-Avi, V., Lang, R. M., Badano, L. P., Belohlavek, M., Cardim, N. M., Derumeaux, G., et al. (2011). Current and evolving echocardiographic techniques for the quantitative evaluation of cardiac mechanics: ASE/EAE consensus statement on methodology and indications endorsed by the Japanese Society of Echocardiography. *European Heart Journal - Cardiovascular Imaging, 12*(3), 167–205. doi:10.1093/ejechocard/jer021.

15. Kobirumaki-Shimozawa, F., Oyama, K., Shimozawa, T., Mizuno, A., Ohki, T., Terui, T., et al. (2016). Nano-imaging of the beating mouse heart in vivo: importance of sarcomere dynamics, as opposed to sarcomere length per se, in the regulation of cardiac function. *The Journal of General Physiology, 147*(1), 53–62. doi:10.1085/jgp.201511484.

16. Reynet, C., & Kahn, C. R. (1993). Rad: a member of the Ras family overexpressed in muscle of type II diabetic humans. *Science, 262*(5138), 1441–1444.

17. Guazzi, M., Dickstein, K., Vicenzi, M., & Arena, R. (2009). Six-minute walk test and cardiopulmonary exercise testing in patients with chronic heart failure: a comparative analysis on clinical and prognostic insights. *Circulation. Heart Failure, 2*(6), 549–555. doi:10.1161/circheartfailure.109.881326.

18. Bijnens, B., Claus, P., Weidemann, F., Strotmann, J., & Sutherland, G. R. (2007). Investigating cardiac function using motion and deformation analysis in the setting of coronary artery disease. *Circulation, 116*(21), 2453–2464. doi:10.1161/circulationaha.106.684357.

19. Hare, J. L., Brown, J. K., Leano, R., Jenkins, C., Woodward, N., & Marwick, T. H. (2009). Use of myocardial deformation imaging to detect preclinical myocardial dysfunction before conventional measures in patients undergoing breast cancer treatment with trastuzumab. *American Heart Journal, 158*(2), 294–301. doi:10.1016/j.ahj.2009.05.031.

20. Nishikage, T., Nakai, H., Mor-Avi, V., Lang, R. M., Salgo, I. S., Settlemier, S. H., et al. (2009). Quantitative assessment of left ventricular volume and ejection fraction using two-dimensional speckle tracking echocardiography. *European Heart Journal - Cardiovascular Imaging, 10*(1), 82–88. doi:10.1093/ejechocard/jen166.

21. Bauer, M., Cheng, S., Jain, M., Ngoy, S., Theodoropoulos, C., Trujillo, A., et al. (2011). Echocardiographic speckle-tracking based strain imaging for rapid cardiovascular phenotyping in mice. *Circulation Research, 108*(8), 908–916. doi:10.1161/CIRCRESAHA.110.239574.

22. Yamada, S., Arrell, D. K., Kane, G. C., Nelson, T. J., Perez-Terzic, C. M., Behfar, A., et al. (2013). Mechanical dyssynchrony precedes QRS widening in ATP-sensitive K+ channel–deficient dilated cardiomyopathy. *Journal of the American Heart Association, 2*(6), doi:10.1161/jaha.113.000410.

23. Haggerty, C. M., Mattingly, A. C., Kramer, S. P., Binkley, C. M., Jing, L., Suever, J. D., et al. (2015). Left ventricular mechanical dysfunction in diet-induced obese mice is exacerbated during inotropic stress: a cine DENSE cardiovascular magnetic resonance study. [journal article]. *Journal of Cardiovascular Magnetic Resonance, 17*(1), 1–14. doi:10.1186/s12968-015-0180-7.

24. Bhan, A., Sirker, A., Zhang, J., Protti, A., Catibog, N., Driver, W., et al. (2014). High frequency speckle tracking echocardiography in

444

J. of Cardiovasc. Trans. Res. (2016) 9:432–444

the assessment of left ventricular function after murine myocardial infarction. *American Journal of Physiology - Heart and Circulatory Physiology.* doi:10.1152/ajpheart.00553.2013.

25. Peng, Y., Popović, Z. B., Sopko, N., Drinko, J., Zhang, Z., Thomas, J. D., et al. (2009). Speckle tracking echocardiography in the assessment of mouse models of cardiac dysfunction. *American Journal of Physiology - Heart and Circulatory Physiology, 297*(2), H811–H820. doi:10.1152/ajpheart.00385.2009.

26. Maillet, M., van Berlo, J. H., & Molkentin, J. D. (2013). Molecular basis of physiological heart growth: fundamental concepts and new players. [10.1038/nrm3495]. *Nature Reviews. Molecular Cell Biology, 14*(1), 38–48.

27. van Berlo, J. H., Maillet, M., & Molkentin, J. D. (2013). Signaling effectors underlying pathologic growth and remodeling of the heart. *The Journal of Clinical Investigation, 123*(1), 37–45. doi:10.1172/JCI62839.

28. Muth, J. N., Yamaguchi, H., Mikala, G., Grupp, I. L., Lewis, W., Cheng, H., et al. (1999). Cardiac-specific overexpression of the alpha(1) subunit of the L-type voltage-dependent Ca(2+) channel in transgenic mice. Loss of isoproterenol-induced contraction.PG - 21503–6. *The Journal of Biological Chemistry, 274*(31), 21503–21506.

29. Chen, X., Nakayama, H., Zhang, X., Ai, X., Harris, D. M., Tang, M., et al. (2011). Calcium influx through Cav1.2 is a proximal signal for pathological cardiomyocyte hypertrophy. *Journal of Molecular and Cellular Cardiology, 50*(50), 460–470. doi:10.1016/j.yjmcc.2010.11.012.

30. Gorski, P. A., Ceholski, D. K., & Hajjar, R. J. (2015). Altered myocardial calcium cycling and energetics in heart failure—a rational approach for disease treatment. *Cell Metabolism, 21*(2), 183–194. doi:10.1016/j.cmet.2015.01.005.

31. Wisløff, U., Loennechen, J. P., Falck, G., Beisvag, V., Currie, S., Smith, G., et al. (2001). Increased contractility and calcium sensitivity in cardiac myocytes isolated from endurance trained rats. *Cardiovascular Research, 50*(3), 495–508. doi:10.1016/s0008-6363(01)00210-3.